This document was prepared in conjunction with work accomplished under Contract No. DE-AC09-96SR18500 with the U. S. Department of Energy.

DISCLAIMER

WSRC-TR-2003-00267, REVISION 0
SRT-RPP-2003-00221, REVISION 0

Key Words:
Cesium eluate,
Physical property models

Retention:
Permanent

Key WTP R&T References:
Test Specification:
24590-WTP-TSP-RT-01-008, Rev. 0
Test Plan: WSRC-TR-2001-00408, Rev. 0
R&T Focus Area: Evaporation
Test Scoping Statements: SS74 & SS79

VALIDATION AND APPLICATION OF CONCENTRATED CESIUM ELUATE PHYSICAL PROPERTY MODELS

A. S. Choi, SRTC
R. A. Pierce, SRTC

DECEMBER 2003

Westinghouse Savannah River Company
Savannah River Site
Aiken, SC 29808

Prepared for the U.S. Department of Energy Under Contract Number DE-AC09-96SR18500

SRS savannah river site ™

TABLE OF CONTENTS

LIST OF FIGURES

LIST OF TABLES

LIST OF ACRONYMS

RPP	River Protection Project
SRTC	Savannah River Technology Center
SS	Scoping Statement
VRF	Volume Reduction Factors
WTP	Hanford Waste Treatment and Immobilization Plant

This page intentionally left blank.

1.0 SUMMARY OF TESTING

The physical property models developed earlier for the concentrated cesium eluate solutions were validated in this work against data taken during recent bench-scale evaporator runs with nonradioactive simulant feeds. The bench-scale data simulated the cesium eluate solutions derived from the ion-exchange processing of AN-102, AN-103, AN-107, AW-101, and AZ-102 supernate. The physical properties that were estimated using the models and compared against measured data included the density, heat capacity, viscosity, and bulk solubility of the saturated eluate solutions at 20 ^{o}C. Since it was difficult to determine the true saturation point with the bench-scale apparatus used, each model prediction was compared with the data taken just prior to and right after the formation of the first solids, which sets the maximum number of model-to-data comparisons that can be made at 40. However, due to missing heat capacity and viscosity data for both AN-102 and AN-103 samples, the actual number of model-to-data comparisons made in this work was 36.

The task acceptance criterion that requires model predictions to be within ±15% of measured data was met in 32 out of the 36 model-to-data comparisons made. Specifically, the predicted densities and heat capacities of the five saturated cesium eluate solutions were found to be all within ±15% of 18 measured data points. For the viscosity, the model predictions were found to exceed the task acceptance criterion for 2 out of 8 measured data points; the model under predicted the viscosities of the AN-103 and AN-107 post-precipitation samples by 24.0 and 21.6%, respectively. However, a closer analysis of data suggested that both discrepancies were likely due to the analytical errors caused by entrained micro-solids impeding the liquid flow through the Cannon-Fenske tube, thereby returning false high viscosity readings.

For the solubility, the model predictions were found to exceed the task acceptance criterion for 2 out of 10 measured data points; the model under predicted the bulk solubilities of both pre- and post-precipitation AN-102 samples by 15.6 and 21.0%, respectively. In fact, the predicted solubilities for the remaining samples were also consistently lower than the measured values, even though the task acceptance criterion was met in each case. This suggests a negative bias within the solubility model, which is thought to be partly due to the questionable prediction by the 6-component nitric acid database used in this work on the partitioning of total acid between dissociated and undissociated acids. However, under prediction of the bulk solubilities by the model would be conservative from the standpoint of precluding the potential for forming any solids during the transfer and storage of concentrated cesium eluate solutions.

It is therefore concluded that the physical property models that were developed as part of the Scoping Statement (SS) 79 requirements adequately predicted measured density, viscosity, heat capacity, and solubility data for the five saturated cesium eluate simulants in 32 of 34 cases, after excluding the two questionable viscosity data points. Furthermore, considering the fact that the two solubility predictions that exceeded the task acceptance criterion were limited only to the AN-102 samples, the models were then used to predict the physical properties of the radioactive AW-101 cesium eluate samples whose major cation concentrations were roughly half of those of the simulant but at a slightly higher acidity.

The density, viscosity, heat capacity, and bulk solubility of the radioactive AW-101 cesium eluate thus predicted at saturation all turned out to be quite similar to those predicted for the nonradioactive counterpart, which indicates that both feeds would lead to the same saturation endpoint. However, saturation was predicted to occur after nearly twice as much radioactive feed as the simulant had been fed. This doubled cumulative feed volume or volume reduction factor for the same saturation endpoint was expected, since each volume of the radioactive feed entering the evaporator pot would contain the same amount of acid as that in the same volume of simulant but only half of the remaining salts. The physical properties and volume reduction factor thus predicted for the saturated radioactive AW-101 cesium eluate were also validated indirectly by comparing the results of the earlier AW-101 simulant test against the new data obtained during this work using the same simulant feed but diluted by a factor of 4.

Since it is not possible to determine the 80% saturation point experimentally, the VRF model proposed earlier for the 80% saturated solutions could not be validated directly against data. Nevertheless, it is recommended that the VRF model in its current form not be used to predict the evaporator endpoint of 80% saturation to support plant operation. This recommendation is made based on the fact that the predicted VRFs for AW-101 and AZ-102 at 80% saturation were higher than those measured for their respective samples under either the pre- or post-precipitation conditions, which is physically not feasible.

This report provides a detailed description of model validation and application efforts made in this work, and issuing this report completes all the requirements of the Scoping Statements 74 and 79.

1.1 OBJECTIVES

This work contained two objectives. The first objective was to complete the remaining requirement of the task plan for the Scoping Statement 79 [Choi, 2001a]:

> To verify the mathematical equations developed for the physical properties of concentrated cesium eluate solutions against experimental test results obtained with simulated feeds.

The second objective was to satisfy the requirements of the Scoping Statement 74:

> To estimate the physical properties of the radioactive AW-101 cesium eluate at saturation using the validated models.

1.2 CONDUCT OF TESTING

The overall task to validate the physical property models of saturated cesium eluate solutions and to further apply the models to the radioactive AW-101 cesium eluate was carried out in the following steps:

A. **Derivation of model input data for simulant runs** – The full compositions of the AN-102, AN-103, AN-107, AW-101 and AZ-102 cesium eluate simulants given elsewhere [Pierce, 2002 & 2003a] were converted into the scaled weight fractions based on the six major cations only, including Al, Ca, Cs, H, K, and Na.

B. **Estimation of physical properties at saturation** – The scaled weight fractions of six major cations derived in Step A were entered into the physical property models derived earlier [Choi, 2003] to estimate the density, viscosity, heat capacity, and solubility of saturated AN-102, AN-103, AN-107, AW-101, and AZ-102 cesium eluate solutions at 20 ^{o}C.

C. **Comparison of model predictions with measured data** – The physical properties estimated in Step B were compared against bench-scale data taken just prior to and right after the formation of the first solids. The conformity to the task acceptance criterion was checked by calculating the difference between predicted and measured values of each property in terms of percent of the measured value.

D. **Derivation of model input data for radioactive run** – The full composition of the most representative radioactive AW-101 cesium eluate sample was derived from available analytical data [Hassan, 2003] and converted into the scaled weight fractions based on the six major cations only, including Al, Ca, Cs, H, K, and Na.

E. **Estimation of physical properties of radioactive cesium eluate** - The scaled weight fractions of six major cations derived in Step D were entered into the physical property models derived earlier [Choi, 2003] to estimate the density, viscosity, heat capacity, and solubility of saturated AW-101 cesium eluate solution at 20 ^{o}C.

F. **Confirmatory testing with diluted AW-101 cesium eluate simulant** – The physical properties of the saturated radioactive AW-101 cesium eluate estimated in Step E were validated indirectly by comparing the existing AW-101 simulant data against the new set of data obtained with a 4X diluted feed.

1.3 RESULTS AND PERFORMANCE AGAINST OBJECTIVES

The task acceptance criterion requires that model predictions be within ±15% of measured data [Choi, 2001a]. It is noted that the criterion was set to coincide with the typical analytical uncertainties on the order of ±15%. In Table 1-1, the conformity of the physical property models to the task acceptance criterion is checked by calculating the degree of deviation of each model prediction from its measured counterpart in terms of percent of each measured property. Since the true saturation point could not be determined experimentally, each model prediction was compared against the data taken just prior to and right after the formation of the first solids for a total of 36 model-to-data comparisons or cases.

Also shown in Table 1-1 are the estimated volume reduction factors (VRF), which represent the cumulative feed volume in multiples of pot volume in a constant-volume evaporator.

Model predictions were within ±15% of measured data in 32 out of the total 36 cases, and those 4 cases of nonconformity are shown in shades in Table 1-1. Specifically, the predicted densities and heat capacities of the five saturated cesium eluate simulants were all within ±15% of 18 measured data points.

For the viscosity, model predictions differed from measured data by more than ±15% in 2 out of 8 cases; the model under predicted the viscosities of the AN-103 and AN-107 post-precipitation samples by 24.0 and 21.6%, respectively. However, both of these discrepancies were attributed to the analytical errors caused by entrained micro-solids impeding the liquid flow through the Cannon-Fenske tube, thereby returning falsely high viscosity readings. This claim is supported by the fact that the AN-103 and AN-107 viscosity samples were taken at the VRFs of 64 and 94, respectively, each of which is 4 higher than the corresponding VRFs when the presence of solids was first detected. This means that both solutions could have been concentrated significantly beyond the saturation point by the time the viscosity samples were taken, thus increasing the likelihood of solids entrainment.

Table 1-1. Deviation of Model Predictions from Measured Data in Percent Measured Data at 20 °C

Envelope	Sample	Density	Viscosity	Heat Capacity	Bulk Solubility
AN-102	pre-precipitation	-3.9%	----	----	-15.6%
	@ VRF	40	----	----	40
	post-precipitation	-9.5%	0.8%	-2.7%	-21.0%
	@ VRF	44	44	44	44
AN-103	pre-precipitation	-1.6%	----	----	-5.0%
	@ VRF	56	----	----	56
	post-precipitation	-4.8%	-24.0%	-0.4%	-8.6%
	@ VRF	60	64	64	60
AN-107	pre-precipitation	4.2%	-11.1%	8.3%	-4.5%
	@ VRF	86	86	86	86
	post-precipitation	2.3%	-21.6%	8.0%	-10.2%
	@ VRF	90	94	94	90
AW-101	pre-precipitation	6.6%	-4.8%	0.9%	-7.2%
	@ VRF	14	14	14	14
	post-precipitation	-3.9%	-4.9%	0.6%	-14.4%
	@ VRF	16	16	16	16
AZ-102	pre-precipitation	4.8%	-12.6%	-0.8%	-4.2%
	@ VRF	40	40	40	40
	post-precipitation	-2.1%	-13.9%	-5.9%	-7.0%
	@ VRF	45	50	50	45

For the solubility, model predictions differed from measured data by more than ±15% in 2 out of 10 cases; the model under predicted the bulk solubilities of both pre- and post-precipitation AN-102 samples by 15.6 and 21.0%, respectively. In fact, although to a lesser degree, the predicted solubilities for the remaining samples were all lower than the measured values. These consistent under-predictions suggest that a negative bias exists in the solubility model. One source for such bias could be an anomaly found in the 6-component nitric acid database used in this work; the current database tends to significantly under-predict the degree of acid dissociation as the total acid content in the pot decreases. Thus, the predicted concentration of undissociated acid would remain high even during the latter part of evaporation, which would continue to promote acid volatilization into the overhead and steady reduction of acidity in the pot. And it is the latter effect that would lead to lower bulk solubility predictions. It is not clear why the discrepancies between predicted and measured solubilities were particularly large for the AN-102 sample. It is, however, noted that under predicted solubilities would be conservative from the standpoint of precluding the potential for forming any solids during the transfer and storage of concentrated cesium eluate solutions.

It is, therefore, concluded that the physical property models developed as part of Scoping Statement 79 requirements adequately predicted measured density, viscosity, heat capacity, and solubility data for the five saturated cesium eluate simulants in 32 out of 34 cases, after excluding the two questionable viscosity data points. Furthermore, since the two solubility predictions that exceeded the task acceptance criterion were limited only to AN-102 samples, the models were next used to predict the physical properties of the radioactive AW-101 cesium eluate samples whose compositions were derived from the data taken during ion-exchange runs in the Intermediate Level Cell of SRTC.

As shown in Table 1-2, the physical properties of the radioactive AW-101 cesium eluate thus predicted at saturation turned out to be quite similar to those predicted for the nonradioactive simulant. This means that despite the fact that the concentrations of the major cations in the radioactive feed were roughly half of those of the simulant but at a slightly higher acidity, the two feeds were predicted to produce nearly the same saturated evaporator bottom. The VRF model predicted that it would take nearly twice as much radioactive feed as the simulant to reach the 80% saturation point with respect to $NaNO_3$ (and the same trend should continue to 100% saturation). Since none of the major cation salts except HNO_3 are volatile, and their relative concentrations are roughly the same in both feeds, this VRF prediction should then lead to nearly the same saturation point for both feeds, as long as the acid profiles of the pot liquid track each other closely throughout the evaporation cycle.

The close tracking of acid profiles has been confirmed by the bench-scale data obtained during this work. To support the overall validation efforts, an evaporation test was conducted using the feed that contained the same molar concentration of acid as that of the baseline AW-101 simulant, but the concentrations of the remaining cations were diluted to one-fourth of their respective cation concentrations in the baseline feed [Pierce, 2003]. The test results showed that the measured VRF for the 4X diluted feed was exactly 4 times that of the undiluted feed, and the measured physical properties at saturation were practically identical for both feeds, which confirm the validity of the model results shown in Table 1-2.

Table 1-2. Estimated Properties of Radioactive AW-101 Cesium Eluate at Saturation at 20 °C

Sample	VRF @ 80% Saturation	Density (g/ml)	Viscosity (cP)	Heat Capacity (cal/g/°C)	Bulk Solubility (g TS/ml)
Radioactive	38	1.3403	2.2931	0.6676	0.5920
Simulant	20	1.3340	2.2026	0.6759	0.5835

1.4 QUALITY REQUIREMENTS

This work was conducted in accordance with the RPP-WTP QA requirements specified for work conducted by SRTC as identified in DOE IWO M0SRLE60. SRTC has provided matrices to WTP demonstrating compliance of the SRTC QA program with the requirements specified by WTP. Specific information regarding the compliance of the SRTC QA program with RW-0333P, Revision 10, NQA-1 1989, Part 1, Basic and Supplementary Requirements and NQA-2a 1990, Subpart 2.7 is contained in these matrices.

The quality assurance plan for the ESP software has been issued [Choi, 2001b]. The most essential element of the software verification and validation (V&V) relevant to this work is on the development of the HNO3DB database, which is discussed elsewhere [Choi, 2003]. The results presented in this report satisfy the requirements outlined in the Task Technical and Quality Assurance Plan for this task [Choi, 2001a]. The task plan specifies that all work described in this report does not invoke the additional RW-0333P QA requirements.

1.5 ISSUES

None

2.0 DISCUSSION

The Hanford River Protection Project (RPP) Hanford Waste Treatment and Immobilization Plant (WTP) is currently being built to extract radioisotopes from the vast inventory of Hanford tank wastes and immobilize them in a silicate glass matrix for eventual disposal at a geological repository. The baseline flowsheet for the pretreatment of supernatant liquid wastes includes removal of cesium using regenerative ion-exchange resins [Olson, 2001]. The loaded cesium ion-exchange columns will be eluted with nitric acid nominally at 0.5 molar, and the resulting eluate solution will be concentrated in a forced-convection evaporator to reduce the storage volume and to recover the acid for reuse [Woodworth, 2002]. The reboiler pot is initially charged with a concentrated nitric acid solution and kept under a controlled vacuum during feeding so the pot contents would boil at 50 ^{o}C. The liquid level in the pot is maintained constant by controlling both the feed and boilup rates. The feeding will continue with no bottom removal until the solution in the pot reaches the target endpoint of 80% saturation with respect to any one of the major salt species present.

One of the critical operating requirements of the eluate evaporator is that the potential for any solids formation in the bottom product must be precluded. To ensure solids-free operation, the bulk solubility of cesium eluate solutions must be determined accurately, and the target evaporation endpoint must set based on this bulk solubility. Once a target endpoint has been determined, the capability to accurately predict the physical properties of cesium eluate solutions concentrated to that target endpoint is desired, since such *a priori* predictive tools would undoubtedly yield valuable information on the design and operation of the eluate evaporator and storage tanks, thereby supplementing or even replacing costly experimental tests.

In an earlier work [Choi, 2001c], the bulk solubilities of the AN-107 cesium and technetium eluate solutions were calculated by developing a semi-batch evaporator model using the OLI/ESP software [ESP, 2002], and the mathematical correlations or models for the density, viscosity, and heat capacity of 80% saturated eluate solutions were developed as a function of temperature only. The test specification for this task then expanded the modeling scope by requiring that the physical property models be developed specifically for the AZ-102 cesium eluate, but as a function of both temperature and unevaporated eluate composition [Longwell, 2001]. Tank AZ-102, categorized as an Envelope B tank, was chosen because it is projected to contain the highest level of soluble cesium among the tanks to be processed during the first 10 years of WTP operation. However, the modeling scope was even further expanded later in the task plan, which required that a set of physical property models be developed that are applicable to Envelope A and C as well as Envelop B cesium eluate feeds at temperatures between 20 and 60 ^{o}C [Choi, 2001a].

A unique feature of the physical property models thus developed is that they were built on the virtual data generated from the statistically designed computer experiments [Choi, 2003]. Therefore, in order to establish any credibility for the models, they must be validated against actual test data; the necessary data were taken during recent bench-scale evaporator tests using simulated cesium eluate feeds [Pierce, 2002 & 2003].

Once the validation of models was complete, thus satisfying the remaining requirement of the Scoping Statement 79, this work was also concerned with applying the validated models to predict the physical properties of the radioactive AW-101 cesium eluate in order to satisfy the requirements of the Scoping Statement 74. This report summarizes the results of validation and subsequent application of the physical property models of the projected WTP cesium eluate solutions covering all waste envelopes.

2.1 PHYSICAL PROPERTY MODELS

The models developed earlier are of the following linear form [Choi, 2003]:

Equation 2-1

$$\begin{aligned} \textit{Physical Property} \;=\; & \beta_1 \cdot [Al^{+3}] + \beta_2 \cdot [Ca^{+2}] + \beta_3 \cdot [Cs^{+}] \\ & + \beta_4 \cdot [H^{+}] + \beta_5 \cdot [K^{+}] + \beta_6 \cdot [Na^{+}] \\ & + \beta_7 \cdot [Al^{+3}] \cdot Temp + \beta_8 \cdot [Ca^{+2}] \cdot Temp \\ & + \beta_9 \cdot [Cs^{+}] \cdot Temp + \beta_{10} \cdot [H^{+}] \cdot Temp \\ & + \beta_{11} \cdot [K^{+}] \cdot Temp + \beta_{12} \cdot [Na^{+}] \cdot Temp \end{aligned}$$

where
$\beta_{1\text{-}12}$ = the model coefficients
[concentrations] = scaled weight fractions based on the six major cations only
Temp = temperature in °C

The values of the model coefficients are given in Table 2-1 for both 80% and 100% saturated cesium eluate solutions with respect to $NaNO_3$. It should be noted that since both the VRF and the bulk solubility are closely related, only one of the two was modeled for either the 80% or 100% saturation case, but not both.

The values of model coefficients given in Table 2-1 were determined by optimizing physical property data calculated from extensive computer runs using a statistically designed matrix of hypothetical feeds as the input [Choi, 2003]. The minimum and maximum concentration ranges of the six major cations given in Table 2-2 along with the temperature range from 20 to 60 ^{o}C formed the factor space of interest in the design of the test matrix. The combined concentration of the remaining minor cations not included in the model ranged from 1.8 to 8.6 wt% of the total cations in the eluate samples considered for the matrix design.

Table 2-1. Coefficients of Equation 2-1 Set by Statistical Analysis Using JMP®

Coeff.	80% Saturation				100% Saturation			
	Density (g/ml)	Viscosity (cP)	Heat Capacity (cal/g/°C)	VRF*	Density (g/ml)	Viscosity (cP)	Heat Capacity (cal/g/°C)	Solubility (g TS/ml)
β_1	1.36176	6.11135	0.53721	**139.01782**	1.48886	12.72718	-0.03378	0.73699
β_2	1.44401	3.03668	0.57243	**48.97029**	1.47408	4.95164	0.38964	0.74161
β_3	1.34916	2.26934	0.58492	**27.90272**	1.50460	3.95236	0.49192	0.69789
β_4	1.30755	2.94761	0.85864	**63.09169**	1.31406	2.14149	0.84166	0.51292
β_5	1.37269	1.59566	0.59123	**54.90814**	1.42237	2.51310	0.46440	0.77862
β_6	1.24086	1.66923	0.78125	**-11.80459**	1.25453	1.38919	0.83926	0.42178
β_7	-0.00244	0.03731	-0.01159	**-3.30647**	-0.00619	-0.07447	0.00287	-0.01693
β_8	-0.00162	-0.04848	0.00036	**-1.07174**	-0.00111	-0.09208	0.00499	-0.00097
β_9	0.00389	0.00220	0.00178	**0.58164**	0.00147	-0.02821	0.00185	0.00599
β_{10}	0.00061	-0.03509	-0.00621	**7.73972**	0.00142	-0.00294	-0.00599	0.00356
β_{11}	0.00270	0.02265	-0.00271	**-0.48689**	0.00209	0.00172	0.00039	0.00590
β_{12}	0.00217	-0.00210	-0.00213	**0.52935**	0.00240	0.00758	-0.00426	0.00559

* Volume Reduction Factor (VRF) is defined as the ratio of cumulative feed volume to initial acid volume.

Table 2-2. Valid Temperature and Concentration Ranges for the Models

	Al^{+3} wt fraction	Ca^{+2} wt fraction	Cs^{+} wt fraction	H^{+} wt fraction	K^{+} wt fraction	Na^{+} wt fraction	Temp (°C)
Min	0.0017	0.0000	0.0036	0.0500	0.0141	0.5834	20
Max	0.1243	0.1597	0.1983	0.3188	0.1309	0.7641	60

The physical property models given in Table 2-1 have the following attributes and constraints:

- All models were derived based on 7.25 M initial acid charge and validated in this work against data taken with 7.5 M initial acid charge. Until further validation is done, their application is not recommended for the initial acid charge below 7 M or above 8 M.

- The coefficients of the VRF model for the 80% saturated solutions are highlighted in **bold**, since they could not be validated against test data, and the results of indirect validation were inconclusive at best. As a result, its application to predict the 80% saturation endpoint in support of plant operation is not recommended (see Section 2.6).

- The solubility model has a negative bias, which is conservative from the standpoint of precluding the potential for solids formation (see Section2.3.4).

2.2 EXPERIMENTAL DATA

Non-radioactive simulant tests were run to generate the necessary data for the model validation [Pierce, 2002 & 2003]. The feeds used in these tests simulated the five cesium eluate samples used earlier to define the ranges of major cation concentrations shown in Table 2-2 for the test matrix design. The compositions of the five simulant feeds thus used to generate the validation data are shown in Table 2-3 in terms of scaled weight fractions of cations only, since nitrate was the only significant anion detected in the cesium eluate samples. It should be noted that of the two scaled weight fraction composition sets, the one that is scaled for the six major cations only (shown in the lower part of Table 2-3) was used as the actual input to the models.

Although the intent was to simulate the five eluate samples used in the test matrix design, the scaled weight fractions of some species in the resulting simulants turned out to be just outside the concentration ranges given in Table 2-2. Those nonconforming species are highlighted in **bold** in Table 2-3, and the percent deviations from their respective maximum or minimum bounds were -1.2% for Na in AN-103, 4.8% for H in AN-107, -0.8% for H in AW-101, and -2.8% for Cs in AZ-102. Here, the positive and negative signs indicate deviations from the maximum and minimum concentration bounds, respectively. Since all these deviations were relatively small and well within the analytical error bounds, they were ignored in this work.

Five simulant solutions with varying concentrations of nitrate salts were evaporated until the solubility limit of $NaNO_3$ was reached. Since the evaporator was operating at 50 ^oC, and the physical properties were to be measured under saturation at 20 ^oC or ambient temperature, the samples of pot liquid were pulled periodically throughout the duration of each test and allowed to cool to look for the presence of any solids. As a result, the model-to-data comparison was made on four physical properties of evaporator bottom samples pulled just prior to and right after the detection of the first solids at 20 ^oC. The properties evaluated include the density, viscosity, heat capacity, and bulk solubility. The data compilation is included as Table 2-4.

Most of the data represented direct measurements from the five semi-batch evaporation tests. In some cases, however, due to the apparent anomaly or unavailability of data at a specific volume reduction factor (VRF) and temperature, some of the data were estimated by trending the remaining data associated with the respective tests. In summary, the reported data in Table 2-4 have the following attributes:

- The density data given for AN-102 (at VRF = 40), AN-103 (at VRF = 56), and AZ-102 (at VRF = 40) do not represent measured values at the respective VRFs. Instead, these data were estimated by interpolation of the data measured at lower and higher VRFs.
- All density data were taken at 20 ^oC, regardless of the presence of solids [Pierce, 2003].
- The viscosity and bulk solubility data were taken at ambient temperature. Although it was reported to be 23 ^oC [Pierce, 2003], ambient temperature in the SRTC laboratory actually ranged from 20 to 24 ^oC during the test. So, the measured viscosity and bulk solubility data were compared directly to the model predictions made at the same temperature of 20 ^oC as was for the density.

- The heat capacity data were extrapolated from the existing data. The original data were measured in the respective samples over the temperature range of 35-80 ^{o}C. These data were then extrapolated back to 20 ^{o}C to obtain the values given in Table 2-4.

- The viscosity data for AZ-102 TFL were measured at 50 ^{o}C, while the samples were at near the solubility limit at 20 ^{o}C. These data were then interpolated back to 20 ^{o}C using the literature correlation [Perry, 1984].

- The percent density deviations were calculated with respective to the difference between the measured density and that of water; using the AN-102 pre-precipitation sample as an example,

$$\%\ Difference \quad = \quad \left(\frac{1.3281 - 1.3415}{1.3415 - 1.0000}\right)(100) \quad = \quad -3.9\%$$

- The percent deviations of the remaining properties were calculated with respective to the measured data; using the AN-102 post-precipitation viscosity as an example,

$$\%\ Difference \quad = \quad \left(\frac{2.894 - 2.871}{2.871}\right)(100) \quad = \quad 0.8\%$$

Table 2-3. Scaled Cation Concentrations of Five Cesium Eluate Simulants

Scaled Weight Fractions of All Cations					
	AN-102 SRTC	**AN-103 SRTC**	**AN-107 PNNL**	**AW-101 PNNL**	**AZ-102 TFL**
Cs	0.0106	0.0602	0.0034	0.0242	0.0034
K	0.0353	0.0377	0.0134	0.1249	0.0143
Na	0.6531	0.5551	0.5936	0.7287	0.7031
Al	0.1181	0.0309	0.0025	0.0460	0.0021
Ni	0.0020		0.0570	0.0010	
Ca	0.0291	0.1518		0.0007	0.0025
Cu	0.0133	0.0042	0.0126	0.0167	0.0013
Fe [1]	0.0078	0.0147	0.0078	0.0052	0.0298
Mg	0.0040	0.0068			0.0001
Zn [2]	0.0018	0.0110	0.0021	0.0044	
H^+	0.1249	0.1276	0.3076	0.0483	0.2405
misc [3]					0.0028
Total	1.000	1.000	1.000	1.000	1.000
anhydrous salt (g/L)	8.34	6.21	2.99	21.45	5.98
HNO3 (M)	0.28	0.24	0.36	0.29	0.52
VRF to precipitation	40-44	56-60	86-90	14-16	40-45
sum of major cations	0.9712	0.9633	0.9205	0.9727	0.9660
Scaled Weight Fractions of Major Cations Only					
	AN-102 SRTC	**AN-103 SRTC**	**AN-107 PNNL**	**AW-101 PNNL**	**AZ-102 TFL**
Al	0.1216	0.0320	0.0027	0.0473	0.0021
Ca	0.0300	0.1576	0.0000	0.0007	0.0026
Cs	0.0109	0.0625	0.0037	0.0249	**0.0035**
K	0.0364	0.0392	0.0146	0.1284	0.0148
Na	0.6725	**0.5762**	0.6449	0.7492	0.7279
H+	0.1286	0.1324	**0.3341**	**0.0496**	0.2490
Total	1.000	1.000	1.000	1.000	1.000

[1] Includes Cr
[2] Includes Pb
[3] Includes Ba, Mn, Si, and Sr

Table 2-4. Comparison of Measured and Calculated Physical Properties at 20 °C

Physical Properties	Density (g/ml)	Viscosity (cP)	Heat Capacity (cal/g/°C)	Solubility (g TS/ml)*
AN-102				
model predictions	1.3281	2.894	0.640	0.546
data (w/o solids)	1.3415	----	----	0.647
VRF (w/o solids)	40	----	----	40
model-data (% data)	-3.9%	----	----	-15.6%
data (w/ solids)	1.3625	2.871	0.658	0.690
VRF (w/ solids)	44	44	44	44
model-data (% data)	-9.5%	0.8%	-2.7%	-21.0%
AN-103				
model predictions	1.3542	2.325	0.660	0.598
data (w/o solids)	1.3600	----	----	0.629
VRF (w/o solids)	56	----	----	56
model-data (% data)	-1.6%	----	----	-5.0%
data (w/ solids)	1.3722	3.058	0.662	0.654
VRF (w/ solids)	60	64	64	60
model-data (% data)	-4.8%	-24.0%	-0.4%	-8.6%
AN-107				
model predictions	1.3192	1.770	0.736	0.556
data (w/o solids)	1.3063	1.991	0.680	0.583
VRF (w/o solids)	86	86	86	86
model-data (% data)	4.2%	-11.1%	8.3%	-4.5%
data (w/ solids)	1.3120	2.256	0.682	0.619
VRF (w/ solids)	90	94	94	90
model-data (% data)	2.3%	-21.6%	8.0%	-10.2%
AW-101				
model predictions	1.3340	2.203	0.676	0.583
data (w/o solids)	1.3133	2.314	0.670	0.629
VRF (w/o solids)	14	14	14	14
model-data (% data)	6.6%	-4.8%	0.9%	-7.2%
data (w/ solids)	1.3477	2.317	0.672	0.681
VRF (w/ solids)	16	16	16	16
model-data (% data)	-3.9%	-4.9%	0.6%	-14.4%
AZ-102 TFL				
model predictions	1.3162	1.722	0.739	0.553
data (w/o solids)	1.3018	1.970	0.745	0.577
VRF (w/o solids)	40	40	40	40
model-data (% data)	4.8%	-12.6%	-0.8%	-4.2%
data (w/ solids)	1.3228	2.000	0.785	0.594
VRF (w/ solids)	45	50	50	45
model-data (% data)	-2.1%	-13.9%	-5.9%	-7.0%

* TS = total solids (nitric acid + nitrate salts)

2.3 VALIDATION RESULTS

The scaled weight fractions of the six major cations given in the lower part of Table 2-3 were entered into Equation 2-1 along with *Temp* = 20 ^{o}C for each physical property estimation, and the resulting model predictions are compared in Table 2-4 with the data measured just prior to and right after the formation of the first solids.

2.3.1 Density

Table 2-4 shows good agreement between the measured densities and the model predictions. All the density predictions met the task acceptance criterion of being within ±15% of measured data; all deviations are within ±10% of measured data for both the nearly-saturated (pre-precipitation) and saturated (post-precipitation) solutions from the five simulant tests. Of particular interest is the fact that some of the data are above the predicted values, while others are below the predicted values. This is an indication that no significant biases are built into the density model.

2.3.2 Heat Capacity

Table 2-4 again shows good agreement between the measured heat capacities and the model predictions. All the heat capacity predictions met the task acceptance criterion; all deviations are within ±10% of measured data for both the nearly-saturated and saturated solutions from the five simulant tests. As with the density data, the fact that some of the data are above the predicted values while others are below the predicted values is an indication that no significant biases are built into the heat capacity model. Also worth noting is that the pre- and post-precipitation heat capacity predictions for the AN-107 and AW-101 samples are almost identical; this trend was expected since heat capacity does not fluctuate rapidly (no parallel comparisons are available for AN-102 and AN-103).

2.3.3 Viscosity

Table 2-4 shows fair agreement between the measured viscosities and the model predictions. The task acceptance criterion was not met in 2 out of 8 model-to-data comparisons; the model under-predicted the viscosities of the AN-103 and AN-107 post-precipitation samples by 24.0 and 21.6%, respectively. However, it can be argued strongly that these large deviations were due to the error in the analytical method. Specifically, the viscosity data for these samples were measured using the Cannon-Fenske tubes which operate on the principle of gravity flow through a capillary tube. And there are indications that micro-solids may have been entrained in the two suspect samples and caused the liquid flow through the Cannon-Fenske tube to be impeded, thereby returning a false high viscosity value.

The basis for this conclusion came from comparing the data for the pre- and post-precipitation AN-107 samples with those for the AW-101 and AZ-102 samples. The data for AW-101 and AZ-102 show little difference in viscosity between the pre- and post-precipitation conditions. This is expected since the viscosity does not vary greatly with marginal variations in salt concentration.

	Viscosity in cP (% Deviation)	
	Pre-precipitation	**Post-precipitation**
AW-101	2.314 (-4.8%)	2.317 (-4.9%)
	@ VRF = 14	@ VRF = 16
AZ-102	1.970 (-12.6%)	2.000 (-13.9%)
	@ VRF = 40	@ VRF = 50
AN-107	1.991 (-11.1%)	2.256 (-21.6%)
	@ VRF = 86	@ VRF = 94

A parallel behavior is observed in the heat capacity data of AW-101 and AN-107:

	Heat Capacity in cal/g/°C (% Deviation)	
	Pre-precipitation	**Post-precipitation**
AW-101	0.670 (0.89%)	0.672 (0.59%)
	@ VRF = 14	@ VRF = 16
AN-107	0.680 (8.29%)	0.682 (7.98%)
	@ VRF = 86	@ VRF = 94

Therefore, one can observe that the viscosity data for the AN-107 pre-precipitation sample closely matched that of AZ-102 at VRF = 40 (in both measured value and deviation from the calculated value). After precipitation, however, something has caused a substantial shift in viscosity (e.g., the presence of micro-solids) in the AN-107 sample. Although no viscosity data is available for the AN-103 pre-precipitation sample, it can be speculated that the likely cause for the substantial shift in viscosity for the AN-107 post-precipitation sample may also be applicable to the AN-103 post-precipitation sample.

2.3.4 Bulk Solubility

Table 2-4 shows good agreement between the measured bulk solubilities and the model predictions. However, the model predictions were found to exceed the task acceptance criterion for 2 out of 10 measured data points; the model under predicted the bulk solubilities of both pre- and post-precipitation AN-102 samples by 15.6 and 21.0%, respectively. A closer analysis of the model trends suggests that these large deviations may be attributable to a bias within the solubility model. This speculation is based on the fact that the predicted solubilities are consistently lower than the measured values for all the samples tested with the deviations ranging from -4 to -21%.

In order to determine the source for this negative bias, the semi-batch evaporation experiment was next modeled with the AN-102 feed so that detailed profiles of pot concentrations such as total acid and $NaNO_3$ could be derived, and the model results for a specific sample could be compared directly against the measured data for the same sample, instead of comparing the results based on the general models given by Equation 2-1 and Table 2-1 that cover all waste envelopes.

In Figure 2-1, the measured concentration profiles of total acid and $NaNO_3$ in the pot are compared with those calculated using the AN-102 model. As expected, both calculated and measured profiles of $NaNO_3$ concentration are shown to increase linearly with the increasing VRF or cumulative feed volume, since $NaNO_3$ is essentially nonvolatile. The difference in slope is mainly due to the difference between the measured and calculated densities of the pot solution, as the total salt content increases. The calculated profile of total acid in the pot is also shown to decrease linearly for the most part from the initial value of 7.5 M to about 3.5 M at saturation with respect to $NaNO_3$. However, the measured acid profile is shown to plateau at ~5 M. Since the total acidity in the pot remained higher during the experiment, it took less feed to saturate the pot compared to the model prediction; the measured VRF was therefore smaller than the calculated value by about 19%.

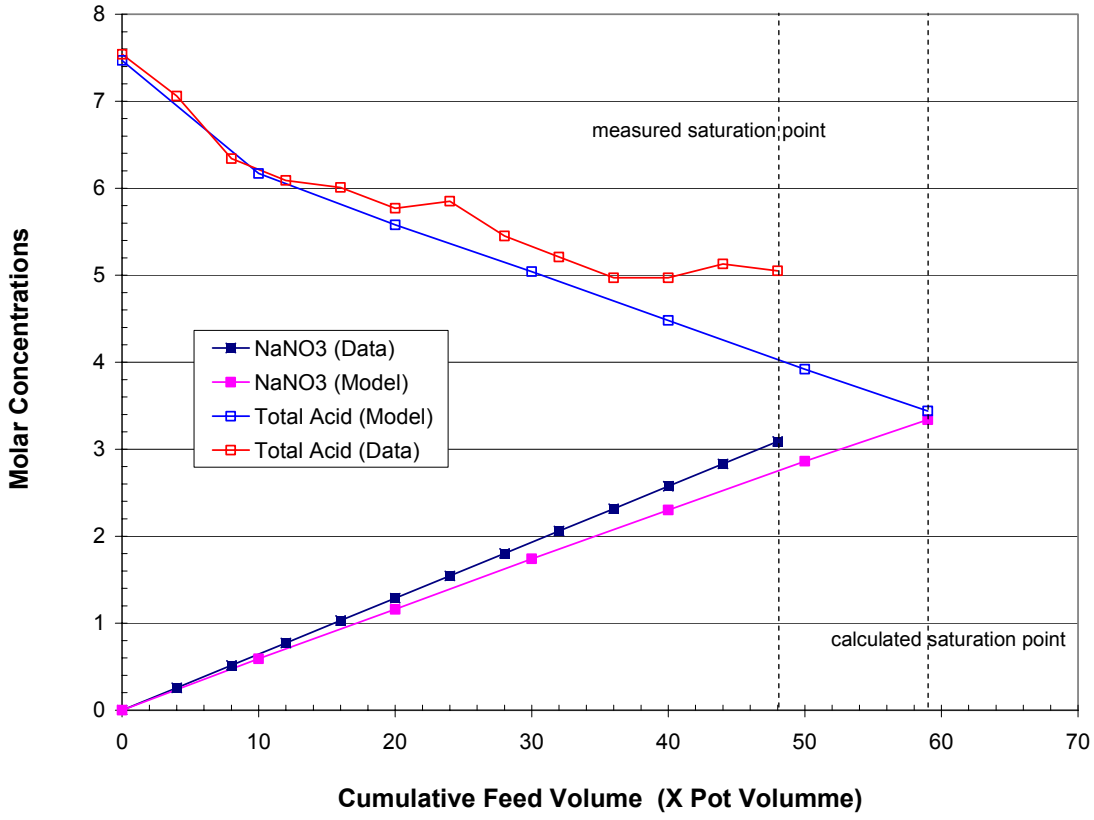

Figure 2-1. Profiles of Total Acid and NaNO3 in the Pot During AN-102 Cesium Eluate Evaporation.

In order to look for the reasons why the predicted acidity in the pot drops off more quickly than the measured values, the predicted partitioning of the total acid between the dissociated and undissociated acids was next plotted in Figure 2-2. The model predicted that 60% of the initial 7.5 M HNO_3 to dissociate into its constituent ions, H^+ and $NO3^-$, while the remaining 40% would dissolve as neutral species, HNO_3 (aq). The percent of dissociated acid is shown to increase during the initial phase of evaporation; however, it is then predicted to decrease steadily, as the total acid content decreases with the increasing salt content in the pot.

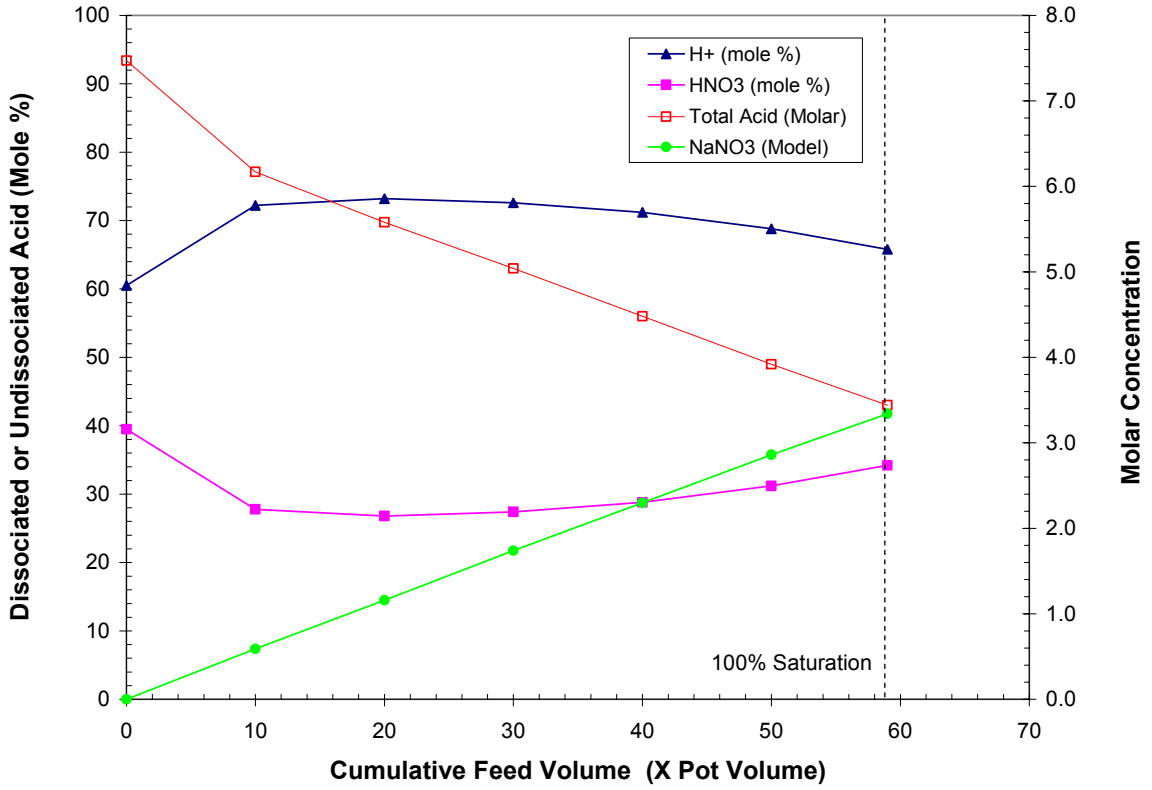

Figure 2-2. Predicted Partitioning of Total Acid During AN-102 Cesium Eluate Evaporation

In the absence of physical entrainment, the emission of nitric acid vapor from an aqueous solution is determined entirely by the following phase equilibrium between the dissolved but undissociated acid and its vapor phase counterpart at the system temperature and pressure:

Reaction 2-1 $HNO_3\,(aq) \leftrightarrow HNO_3\,(g)$

The undissociated nitric acid molecule is further in equilibrium with its constitutive ions in the liquid phase:

Reaction 2-2 $HNO_3\,(aq) \leftrightarrow H^+ + NO_3^-$

Therefore, the predicted trend of decreasing acid dissociation with decreasing acid content shown in Figure 2-2 would shift the equilibrium reaction (Reaction 2-2) to the left, which would in turn shift the equilibrium reaction (Reaction 2-1) to the right, thereby increasing the acid volatilization into the overhead. As a result, the acid content in the pot will continue to drop, contrary to the data trend of leveling off at ~5 M. This means that one way to match the experimental acid profile is to reverse the general trend of decreasing acid dissociation during the latter phase of evaporation, which would then result in reduced acid volatilization to prevent steady drop-off in the pot acidity.

For the HNO_3-H_2O binary system, this desired trend of increasing acid dissociation with decreasing acidity is indeed thermodynamically consistent. In the case of multi-component cesium eluate evaporation, however, the nitrate ions that counterbalance the metal ions will continue to accumulate in the pot throughout the evaporation cycle, which would seem to result in reduced acid dissociation by shifting the equilibrium reaction (Reaction 2-2) to the left. However, the data have shown that the nitrate ions counterbalancing H^+ will still dominate in the evaporation of WTP cesium eluate solutions at the starting acidity of ~7.5 M in the pot [Pierce, 2003].

The AN-102 data shown in Figure 2-1 are re-plotted in Figure 2-3 in terms of total acidity vs. $NaNO_3$. Also shown is the solubility curve for the $NaNO_3$-HNO_3-H_2O ternary system. The measured total acidity in the pot is again shown to level off at ~5 M HNO_3. It is also shown that the solution would become saturated with $NaNO_3$, when the measured total acid profile intersects the ternary solubility curve. It is noted that the AN-102 model also predicted $NaNO_3$ to be the first solid species to form at the VRF of 58. However, the calculated total acid profile is not shown to intersect the ternary solubility curve before saturation is predicted to occur at 3.5 M HNO_3.

The physical properties of the saturated AN-102 cesium eluate were calculated from the AN-102 model results, and the calculated properties are compared in Table 2-5 with the pre- and post precipitation data given in Table 2-4. The calculated bulk solubilities are now within ±15% of both data points, thus satisfying the task acceptance criterion. On the other hand, the new viscosity prediction is considerably lower than either the post-precipitation data or the earlier model prediction, thus exceeding the task acceptance criterion. However, since all of the post-precipitation viscosity data are suspect due to likely interference by entrained micro-solids, it cannot be concluded with certainty that this low viscosity prediction is indeed outside the task acceptance criterion without first comparing it with the pre-precipitation data. In summary, these comparisons seem to suggest that part of the discrepancies shown in Table 2-4 can be attributed to the use of the general property models that cover all the waste envelopes, in lieu of using individual models specifically designed for each waste tank or envelope.

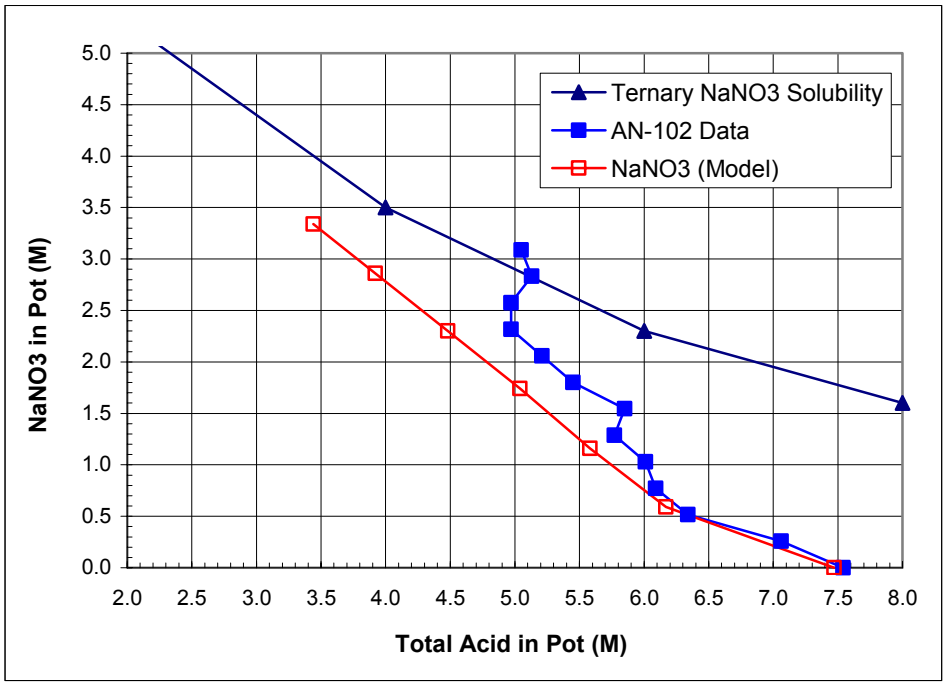

Figure 2-3. Total Acid vs. $NaNO_3$ During AN-102 Cesium Eluate Evaporation

Table 2-5. Comparison of Measured and Calculated Physical Properties of Saturated AN-102 Cesium Eluate at 20 °C

Physical Properties	Density (g/ml)	Viscosity (cP)	heat capacity (cal/g/°C)	Solubility (g TS/ml)
AN-102 model @ VRF = 58	1.3419	2.129	0.660	0.595
data (w/o solids) @ VRF = 40	1.3415	----	----	0.647
model-data (% data)	0.0%	----	----	-8.0%
data (w/ solids) @ VRF = 44	1.3625	2.871	0.658	0.690
model-data (% data)	-1.5%	25.8%	0.3%	-13.8%

2.4 APPLICATION OF MODELS

In the previous section, it was shown that the physical property models given by Equation 2-1 and Table 2-1 adequately predicted measured density, viscosity, heat capacity, and solubility data for the five saturated cesium eluate solutions in 34 out of 36 model-to-data comparisons. Furthermore, since the two solubility predictions that exceeded the task acceptance criterion were limited only to the AN-102 samples, the models were next used to predict the physical properties of the radioactive AW-101 cesium eluate, thereby substituting for the potentially costly evaporation tests in the cells and subsequent property determinations.

2.4.1 Composition of Radioactive AW-101 Cesium Eluate

The radioactive AW-101 cesium eluate samples were taken during recent ion-exchange runs in the Intermediate Level Cell of SRTC, and their analytical data were used as the basis for developing the baseline composition in support of the Scoping Statement 74. The data given in Table 2-6 through Table 2-8 came from Ref. [Hassan, 2003]; only cesium eluate data from Cycles 1 to 5 were used because of excessive dilution in Cycle 6. The cesium data given in Table 2-7 are based on the ^{137}Cs activity of 86.6 Ci/g and the measured feed ^{137}Cs distribution of 26% of total Cs.

Table 2-6. Bed Volume Data for Radioactive AW-101 Cesium Ion-Exchange Runs

	Cycle 1	Cycle 2	Cycle 3	Cycle 4	Cycle 5
Single Bed Volume (mL)	11.7	13.8	12.2	11.9	11.1
Total Liquid Collected (mL)	145	220	186	178	211
Total Bed Volumes	12.4	15.9	15.2	15.0	19.0

Table 2-7. Cesium Data for Radioactive AW-101 Cesium Eluate

	Cycle 1	Cycle 2	Cycle 3	Cycle 4	Cycle 5
^{137}Cs (μCi/mL)	1740	2190	2060	2340	1590
Total Cs (μg/mL)	77.3	97.3	91.5	104	70.6

Considering that most of the cesium was eluted in 8 to 10 bed volumes, the following assessments were made on the data:

- The combination of the cesium and bed volume data suggests that cycles 2 to 4 are quite comparable.
- Cycle 1 appears to exhibit some resistance to cesium elution as evidenced by the relatively low total cesium concentration, even though the value of Total Bed Volumes is low.
- Cycle 5 data would be comparable to that of Cycles 2 to 4 if it had not been diluted out to a total of 19.0 Bed Volumes.
- For Cycle 5, to bring it in line with Cycles 2 to 4, adjusting the Total Bed Volumes to 15.5 yields an adjusted total Cs of 86.5 μg/mL.
- The total Cs value for Cycles 2 through 5 at a nominal Total Bed Volumes value of 15.5 averages 94.8 μg/mL.

Table 2-8. Other Major Cation Data for Radioactive AW-101 Cesium Eluate

	Cycle 1	Cycle 2	Cycle 3	Cycle 4	Cycle 5
Al (μg/mL)	<298	<309	<306	<284	<294
Ca (μg/mL)	<120	<115	<123	<115	<119
K (μg/mL)	<4910	<5090	<5380	<4680	<4840
Na (μg/mL)	1590	1950	1620	1950	1540

The average value for Na is calculated to be 1730 μg/mL. The lack of measurable quantities for Al, Ca, and K complicates the analysis. As a result, previous work with AW-101 was used for comparison and further to develop a recommendation for relative amounts of each element. The data given in Table 2-9 came from a system containing nitrate as the only anion.

Table 2-9. Comparison of Major Cation Data and Proposed Values for Radioactive AW-101 Cesium Eluate

	Cs	Na	Al	Ca	K	H
Ref. [Pierce, 2003]						
(μg/mL)	148	4460	282	4	764	n/a
(mol/liter)	0.0011	0.1939	0.0104	0.0001	0.0195	0.2892
Ref. [Hassan, 2003]						
(μg/mL)	86.5	1760	n/a	n/a	n/a	n/a
(mol/liter)	0.0006	0.0765	n/a	n/a	n/a	n/a
PROPOSED						
(μg/mL)	86.5	1760	135	1.9	367	n/a
(mol/liter)	0.0006	0.0765	0.0050	<0.0001	0.0094	n/a

Several items are worth noting. The data from Ref. [Pierce, 2003] for Al, Ca, and K are below the detection limits cited in Ref. [Hassan, 2003]. There is also some general agreement in the relative amounts of Cs and Na present in each reference. Consequently, it seems that reasonable values for Al, Ca, and K can be proposed for this work using the data from Ref. [Pierce, 2003].

Using an average ratio for the data from the two references, a multiplication factor of 0.48 (based on 0.58 for Cs and 0.39 for Na) was applied to the data from Ref. [Pierce, 2003a] to arrive at the proposed values for Al, Ca, and K.

Nitrate data can then be used to determine a representative value for H^+. The total moles of nitrate present for the AW-101 test in Ref. [Pierce, 2003] can be determined by adding the appropriate amounts in Table 2-9, after making proper allowances for Al (3 moles of nitrate per mole of Al) and Ca (2 moles of nitrate per mole of Ca). The value for nitrate thus calculated was 0.1016 mole/liter.

The total nitrate data for the radioactive AW-101 eluate samples are shown in Table 2-10. Although more speculative than the above assessments, it appears as though an anomaly is present in the measurements for Cycles 3 and 4. The reasons for this assessment are:

- The great similarity among the values for Cycles 1, 2 and 5
- The fact that elution was performed with 0.5 M HNO_3
- The data for Cycles 1, 2 and 5 are consistent with the use of 0.5 M HNO_3 for elution
- An average nitrate value for Cycles 1, 2 and 5 is 0.446 mole/liter

The total nitrate for the proposed composition of Table 2-9, not counting H^+, is 0.1016 moles/liter. Subtracting this value from the average total nitrate value for Cycles 1, 2, and 5 in Table 2-10 (including H^+) yields a proposed H^+ value of 0.344 mole/liter, or 348 μg/mL.

Table 2-10. Nitrate Data for Radioactive AW-101 Cesium Eluate Samples

	Cycle 1	Cycle 2	Cycle 3	Cycle 4	Cycle 5
NO_3^- (mol/liter)	0.448	0.429	0.792	0.631	0.461

Compiling all of the above data, not accounting for other minor cations that are in solution, yields the proposed composition of Table 2-11.

Table 2-11. Proposed Composition of AW-101 Cesium Eluate (all Nitrate Salts)

	Cs	Na	Al	Ca	K	H	Others
(μg/mL)	86.5	1760	135	1.9	367	348	104.2
(mol/liter)	0.0006	0.0765	0.0050	<0.0001	0.0094	0.3444	----
Wt. Fraction w/o Others	0.032	0.652	0.050	0.001	0.136	0.129	----
Wt. Fraction All Elements	0.031	0.628	0.048	0.001	0.131	0.124	0.037

The amounts of "other" elements that ought to be included in a proposed AW-101 composition are difficult to determine using only the data of Ref. [Hassan, 2003]; due to high dilution factors, many of the detection limits are high. At the same time, many "other" compounds were measured in concentrations that are much higher than would be anticipated based on knowledge of the tanks and expected performance of the ion exchange resins. Therefore, additional data were drawn in from two other reports for comparison: BNFL-RPT-014 and SRTC-BNFL-019. The data are listed in Table 2-12.

Comparing the data in Table 2-12 clearly show that the values given in Ref. [Hassan, 2003] are artificially high for B, Ba, Cd, Cr, Cu, La, Li, Ni, Sn and Sr. Experience strongly suggests that the value for Ce is caused by ICPES signal interference from another element such as uranium or plutonium. Therefore, two reports exist for proposing the composition of "other" elements. Due to the way the experiments for the two reports were performed, the data from BNFL-RPT-014 is judged to be the best data for these assumptions. The exception to the data is the likelihood that the B or Si values are artifacts from dissolution of glass equipment and sample vials.

Consequently, the following concentrations are proposed as part of "other" elements:

	(μg/mL)
Ba	0.4
Cd	0.3
Cr	3.5
Cu	50.6
Fe	12.3
Mn	0.7
Ni	5.9
P	2.9
Pb	15.6
Zn	12

The total concentration of these "other" species equals 104.2 μg/mL, and this value has been incorporated in Table 2-11.

Table 2-12. Concentration of Other Elements in Cesium Eluate

	Element Concentration (μg/mL)		
Element	**[Hassan, 2003]**	**[Hassan, 1997]**	**[Kurath, 2000]**
Al	<309	568.7	141.0
B	649.7	3.2	72.6
Ba	99.5	0.4	0.4
Ca	<123	3.5	2.1
Cd	21.9	0.5	0.3
Ce	304.5	nm	nm
Cr	31.3	2.3	3.5
Cu	146.1	11.5	50.6
Fe	18.8	4.8	12.3
K	<5380	923.0	382.0
La	49.6	3.0	<0.3
Li	224.7	0.9	nm
Mg	<26.4	0.4	<1.1
Mn	<4.3	0.5	0.7
Mo	<287	4.2	<0.3
Na	1760.0	5706.2	2230.0
Ni	70.5	3.6	5.9
P	<374	9.8	2.9
Pb	<173	7.6	15.6
Si	<87.2	11.1	51.4
Sn	375.1	3.1	<10.7
Sr	39.7	<0.2	nm
Ti	<40.2	0.8	<0.1
Zn	<17.3	1.1	12.0
Zr	<124	1.0	nm

2.4.2 Estimation of Radioactive AW-101 Cesium Eluate Properties

The scaled weight fractions of the six major cations given in Table 2-11, not including the other species, were entered into Equation 2-1 along with *Temp* = 20 ^{o}C for each physical property estimation. The resulting model predictions are compared in Table 2-13 with those predicted earlier for the non radioactive simulant. It turned out that all four predicted properties of both radioactive and non radioactive AW-101 cesium eluate at saturation are quite similar, which means that despite the significant differences in the major cation concentrations, the two feeds will produce nearly the same saturated evaporator bottom. It is worth noting that the model also predicted it would take almost twice as much volume of the radioactive feed as the simulant to reach the same 80% saturation point (and the same trend should continue to 100% saturation).

Table 2-13. Estimated Properties of Radioactive AW-101 Cesium Eluate at Saturation at 20 ^{o}C

Sample	VRF @ 80% Saturation	Density (g/ml)	Viscosity (cP)	Heat Capacity (cal/g/^{o}C)	Bulk Solubility (g TS/ml)
Radioactive	38	1.3403	2.2931	0.6676	0.5920
Simulant	20	1.3340	2.2026	0.6759	0.5835

In order to investigate the reasons for the near identical endpoints, the compositions of the two eluate feeds are compared in Table 2-14. It is clearly seen that the radioactive feed is only about half as concentrated as the simulant, when the total salt contents of both feeds, including the acid, are compared. Specifically, the concentrations of all major cations, except H^{+}, are shown to be 40-60% of their respective counterpart in the simulant. However, the acid concentrations are seen to be comparable in both feeds. Since none of the major cation salts except HNO_3 are volatile, they will continue to accumulate in the pot throughout the evaporation cycle. Therefore, when the predicted VRF for the radioactive feed is nearly twice as high as that for the simulant, the total salt accumulation in the saturated bottom will be nearly identical for both feeds, provided that the profiles of pot acidity for both feeds track each other closely. The close tracking of acid profiles has been confirmed in a bench-scale test conducted in parallel during this validation work, which is described in the next section.

Table 2-14. Comparison of Radioactive and Simulated AW-101 Cesium Eluates

	Rad. (mg/L)	Sim. (mg/L)	Rad.-Sim. (% Sim.)	2X Rad. (mg/L)	Rad. (swf)	Sim. (swf)	Rad./Sim. (swf/swf)
Al	135	281.5	-52.0	270	0.050	0.047	1.1
Ca	1.9	4.0	-52.4	3.8	0.001	0.001	1.5
Cs	86.5	148.0	-41.6	173	0.032	0.025	1.3
H	348	295.2	17.9	696	0.129	0.050	2.6
K	367	764.0	-52.0	734	0.136	0.128	1.1
Na	1,760	4,458.1	-60.5	3,520	0.652	0.749	0.9
Others	104.2	166.7	-37.5	208.4			
Total	2,802.6	6,117.5		5,605.2	1.000	1.000	

2.5 CONFIRMATORY TESTING

A bench-scale evaporator test was conducted as part of the overall validation efforts to confirm the model predictions on the radioactive AW-101 cesium eluate which were discussed in the previous section. Both experimental procedure and results are presented in this section.

2.5.1 Preparation of Cesium Eluate Simulant

The baseline AW-101 cesium eluate simulant was prepared earlier according to the batch sheet shown in Table 2-15 to support this study [Pierce, 2003]. The mass of each constituent species added to the baseline simulant is shown to be different from those used earlier solely due to the difference in the final simulant volumes made. Also shown in the table is the recipe for the 4X diluted AW-101 simulant used in this test. All salts were weighed on a calibrated balance. Nitric acid volumes were measured using a graduated cylinder whose markings had been validated with weighed deionized water. The final volume for the simulant was obtained by diluting with deionized water. Visual inspection of the final solutions confirmed that all solids had dissolved.

2.5.2 System Configuration

A schematic of the experimental setup is shown in Figure 2-4. The evaporator, feed reservoir, mist eliminator, and condensers were fabricated in the SRTC Glass Shop. The evaporator is a 5-inch diameter glass vessel with a volume of 2200 mL. Heating is supplied through a Fisher Scientific IR4100 infrared hot plate. The evaporator is wrapped with an insulation blanket and has glass beads in the bottom to act as boiling stones. Feed is drawn into the evaporator by the vacuum in the system and is regulated through a metering stopcock. The temperature of the evaporator contents is monitored using a Cole-Parmer Type J thermocouple and thermocouple readout. The evaporator pressure is measured using a calibrated Omega Engineering PX01C1-O20AI high-accuracy pressure transducer attached to an Omega DP41-E meter. An air bleed valve is attached to the evaporator top to control the evaporator pressure.

Table 2-15. AW-101 Cesium Eluate Simulant Batch Sheet

Simulant	Baseline AW-101	AW-101 4X Dilution
Nitrate Salt		
$CsNO_3$ (g)	2.171	0.868
KNO_3 (g)	19.755	7.902
$NaNO_3$ (g)	164.807	65.923
$Al(NO_3)_3$-$9H_2O$ (g)	39.180	15.672
$Ni(NO_3)_2$-$6H_2O$ (g)	0.297	0.119
$Ca(NO_3)_2$-$4H_2O$ (g)	0.236	0.094
$Cu(NO_3)_2$-$2.5H_2O$ (g)	3.736	1.494
$Fe(NO_3)_3$-$9H_2O$ (g)	2.282	0.913
$Zn(NO_3)_2$-$6H_2O$ (g)	1.235	0.494
15.7M HNO_3 (mL)	184.2	294.8
HNO_3 (M)	0.30	0.30
Final Volume (liters)	10.0	16.0

Condenser #1 is a 4-inch diameter vessel that is approximately 19 inches tall. Cooling coils extend 12 inches down into the vessel. The liquid volume below the coils is 1200 mL and the volume below the gas inlet tube is 1400 mL. Condenser #1 is cooled using a Neslab RTE-211 chiller. Condensate is removed from the system using a Fluid Metering, Inc. Model QV Pump.

Condenser #2 is a 4-inch diameter vessel that is approximately 14.5 inches tall. Cooling coils extend 13.5 inches down into the vessel. The liquid volume below the coils is 150 mL and the volume below the gas inlet tube is 300 mL. Condenser #2 is cooled using a Lauda E200 chiller. Condensate is removed from the system using a Fluid Metering, Inc. Model QV Pump.

Vacuum is pulled on the system using a Vacuubrand MZ 2C Pump. Condensate conductivity is measured using a YSI 3200 Conductivity Meter equipped with a YSI Type 3253 Glass Dip Cell. Titrations performed in the lab use certified 0.0050-0.010M NaOH with endpoint determined using phenolphthalein indicator.

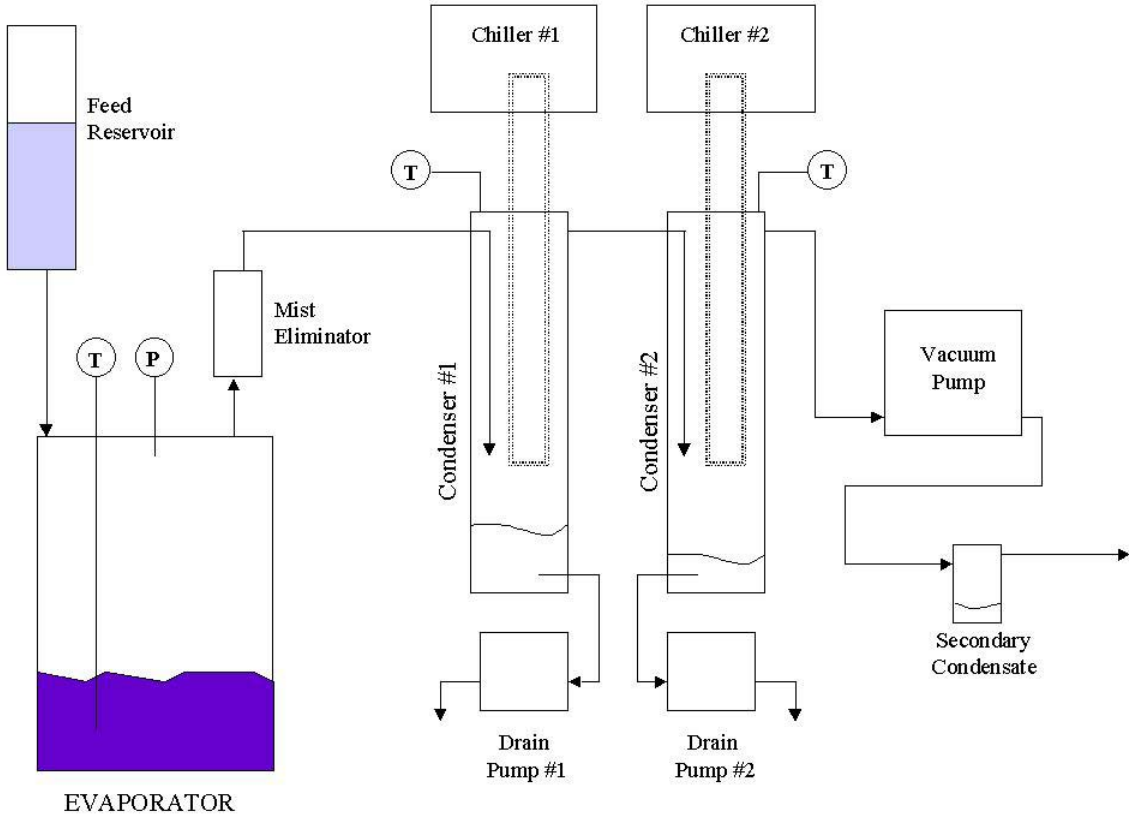

Figure 2-4. Schematic of the Bench-Scale Evaporator Unit Used in this Work

2.5.3 Experimental Procedure

The semi-batch evaporation test was conducted as follows. The evaporator pressure was kept at 70±3 torr. The starting pot volume was 250 mL containing 7.5M HNO_3. The evaporator pot was marked with a line to indicate the initial operating volume. As samples were withdrawn, the line was moved to reflect the adjusted volume. The evaporation rate used for the test was approximately 12.5 mL/min. This corresponds to one evaporator pot volume (250 mL) every 20 minutes.

The first chiller was operated at 20°C and the second chiller at 10°C. These chillers were operated at temperatures below the RPP design values in order to minimize the amount of condensate lost from the system so that the measured condensate acidity closely reflects the composition of what was evaporated. The other primary controls were the evaporator pot and feed volumes. Temperatures in the evaporator pot and first condenser were monitored with thermocouples.

The test was performed at a rate of approximately 16-20 evaporator volumes per day – eight in the morning and 8-12 in the afternoon. After each set of four evaporator volumes, the vacuum was removed from the system and the condensers were emptied. Any liquid collected in the mist eliminator was charged back into the pot. During the test, samples were periodically taken to analyze for density (10 mL) and total acid by titration (0.10-0.15 mL). The density sample is not altered by the analysis and, therefore, was returned to the evaporator pot. No foaming problems were encountered during evaporation.

A conductivity probe measured evaporator condensate acidity. The conductivity probe was checked against three known HNO_3 solutions – 0.20M, 0.40M, and 0.80M – prior to analysis of condensate samples. The condensate from Condensers #1 and #2 were combined prior to analysis. After being mixed, the combined condensate was analyzed for conductivity. Several conductivity results were validated using a titration method. Secondary condensate from each day was also collected and the volume was noted.

At the appropriate time, as saturation was approached, samples were removed and stored to look for precipitation. Samples were removed at volume reduction factors (VRF) of 14 and 16. When samples were removed, the feed and pot control volumes were adjusted to compensate for the withdrawn sample. Upon cooling, these samples were inspected for solids. The evaporation sequence was continued until precipitation was observed in the evaporator pot sample that had cooled to room temperature.

All intermediate samples were analyzed for density at 20^{o}C using an Anton-Paar DMA 4500 density meter. The density meter is accurate to 0.0001 g/cm^3. Prior to analyzing samples, the instrument calibration is verified using deionized water. The samples are injected into the instrument, the instrument adjusts the sample temperature to 20^{o}C, and the sample is analyzed. Intermediate samples were also analyzed for total acid (by titration) and viscosity. Viscosity was determined from the average of triplicate measurements using calibrated Cannon-Fenske Size 50 viscometers (sized for approximate viscosity of 1-5 cp). Primary condensate samples were analyzed for acid concentration using conductivity.

2.5.4 Discussion of Results

The exact point of saturation was difficult to determine instantly because the solution was evaporated at 55^{o}C and then had to be cooled to room temperature to determine the saturation point at 20 ^{o}C. Therefore, the potential for super saturation was high. The best way to identify the approximate saturation point was to withdraw intermediate samples as the saturation point was approached and allow sufficient time for the samples to precipitate. Since the primary salt to precipitate out was $NaNO_3$, the end point for each run was estimated using the ternary $NaNO_3$-HNO_3–H_20 solubility data. The HNO_3 concentration was measured using acid-base titration. Because of vigorous boiling in the evaporator pot, the total acid value can vary as much as $\pm$10% due to difficulty in maintaining a constant volume, although $\pm$5% is more likely.

Measured concentrations of $NaNO_3$ and HNO_3 during the course of the test are shown in Table 2-16. Because the system contains only nitrate salts, $NaNO_3$ is represented in the table as Na^+ and HNO_3 is represented as H^+. The data show that precipitates were first detected in the pot sample taken at VRF = 58, i.e., when the cumulative volume of diluted AW-101 simulant fed to the pot was equal to 58 times the pot volume. At that point, the concentration of Na^+ in the pot was 2.8 M at the measured acidity of 5.3 M.

Table 2-16. $NaNO_3$-HNO_3 Evaporation Data

AW-101-7.5M 4X Dilution			
VRF	**H^+ (M)**	**Na^+(M)**	**Condensate H^+ (M)**
0	7.50	0	----
4	----	0.194	0.292
8	7.20	0.388	0.508
12	----	0.582	0.290
16	6.51	0.776	0.321
20	----	0.970	0.278
24	----	1.163	0.385
28	6.48	1.357	0.285
32	----	1.551	0.315
36	6.05	1.745	0.455
40	----	1.939	0.348
44	----	2.133	0.376
50	5.46	2.424	0.353
54	5.43	2.618	0.402
58	**5.33**	**2.812**	**0.318**

Note: AW-101 feed acidity was measured to be 0.309M using conductivity

The acid and Na concentration data given in Table 2-16 were plotted next in Figure 2-5 along with the experimental solubility curve for $NaNO_3$ in the $NaNO_3$-HNO_3-H_2O ternary system. Also plotted are the acid and Na concentration data from the earlier test with the undiluted AW-101 simulant [Pierce, 2003]. The open symbols of Figure 2-5 represent those data points where precipitation occurred. It can be clearly seen that the acid-vs.-salt concentration profiles of both 4X diluted and undiluted feeds are essentially identical. That is, regardless of whether the feed was diluted or not, the two acid profiles tracked each other closely, and the process performance did not change.

In addition, the acid-vs.-salt concentration profiles are shown in Figure 2-5 to intersect the ternary solubility curve of $NaNO_3$ just prior to the precipitation, i.e., when the pre-precipitation samples were taken at VRFs = 54 and 14 for the 4X diluted and undiluted feeds, respectively. It is noted that the VRF ratio of the diluted to undiluted feed is calculated to be 3.9, which is very close to the dilution ratio of 4 used in this test. This confirms the validity of the model prediction discussed in the previous section; the predicted VRF of 38 for the radioactive AW-101 cesium eluate at 80% saturation was nearly twice that of the simulant (VRF = 20), when its major cation concentrations were roughly half of their respective counterparts in the simulant at a comparable acidity.

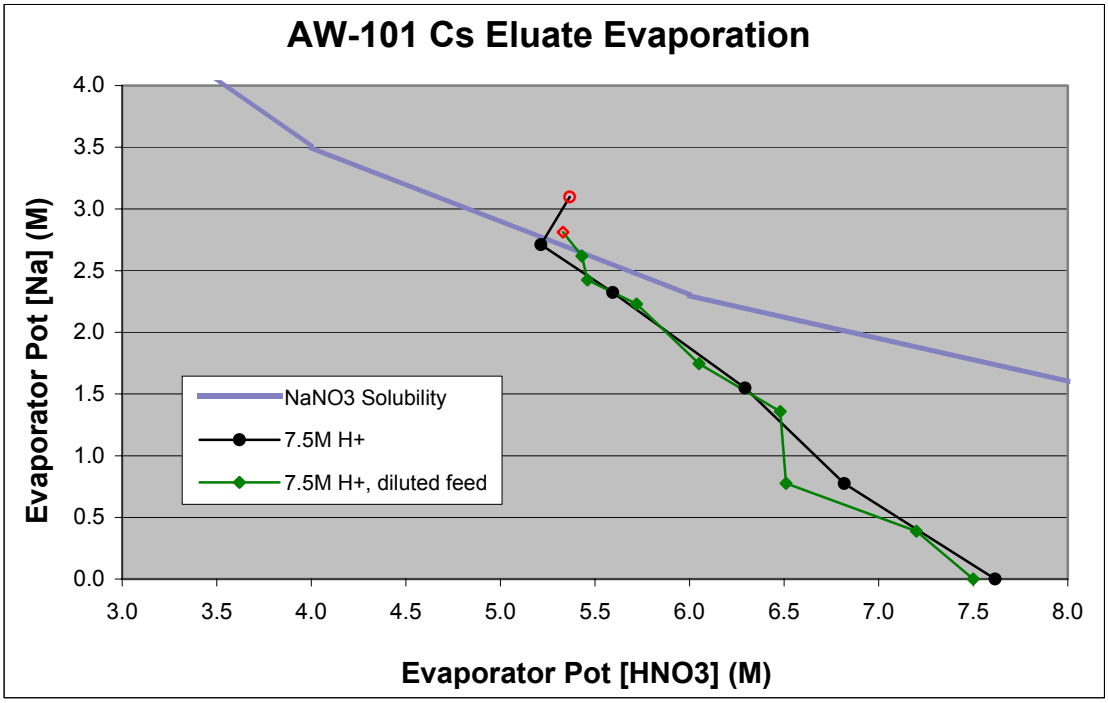

Figure 2-5. Matrix Behavior during AW-101 Cs Eluate Semi-Batch Evaporation

2.5.5 Physical Properties of Diluted AW-101 Cesium Eluate

In addition to the bulk solubility, the density and viscosity data were also collected during this test to see if the final saturated solution would be any different than that derived earlier from the undiluted feed. Density samples were collected throughout the test, and the resulting data at 20°C are compared in Table 2-17 with those obtained earlier with the undiluted feed. When the measured density for the undiluted feed sample taken at a specific VRF is compared to that measured for the 4X diluted feed sample taken at 4 times the VRF of undiluted samples, it can be shown that the absolute difference between the two density data sets is less than 5%, which is within the experimental error bounds.

Table 2-17. Comparison of AW-101 Density Profiles

AW-101-7.5M Undiluted			AW-101-7.5M 4X Dilution		
VRF	**H+ (M)**	**Density (g/mL)**	**VRF**	**H+ (M)**	**Density (g/mL)**
0	7.62	----	0	7.50	----
4	6.82	----	8	7.20	1.2490
8	6.29	1.2599	16	6.51	1.2409
12	5.59	1.3217	28	6.48	1.2650
14	5.21	1.3133	36	6.05	1.2811
16	5.37	1.3477	44	----	1.2881
			50	5.46	1.3178
			54	5.43	1.3356
			58	5.33	1.3260

Few samples were analyzed for viscosity because of the inability to take large quantities of samples repeatedly throughout the experiment. Therefore, only two pot samples were taken in each test – the final solution containing few precipitates and the one just prior to the saturation point. The resulting viscosity data are shown in Table 2-18 along with the density data for the 4X diluted and undiluted AW-101 simulant feeds. As with density, the absolute difference between the measured viscosities of diluted and undiluted feeds is less than 8% for both pre- and post-precipitation samples, which is well within the experimental error bounds.

Table 2-18. Comparison of Physical Property Data at Saturation

Sample #	Temp (deg C)	Density (g/mL) before precipitation	Density (g/mL) after precipitation	Viscosity (cP) before precipitation	Viscosity (cP) after precipitation
AW101-7.5M 4X Dilution	20	1.3356	1.3260	2.15	2.42
AW101-7.5M Undiluted	20	1.3133	1.3477	2.31	2.32
Difference (% 4X Dilution)		-6.3%	6.7%	7.4%	-4.1%

These results of practically identical acid profiles (Figure 2-5) and physical properties (Table 2-18) suggest that the solution in the evaporator pot for the 4X diluted feed case is essentially identical to that of the undiluted feed case from the beginning to the end of evaporation cycle, when it is finally saturated with $NaNO_3$. Therefore, the validity and consistency of the model predictions shown in Table 2-13 for the radioactive AW-101 cesium eluate are confirmed by the data collected under comparable test conditions.

2.6 VOLUME REDUCTION FACTOR

All four physical property models that were developed for the saturated cesium eluate solutions as part of the Scoping Statement 79 requirements have been validated in this work against data obtained with simulated feeds. During the course of discussing the results of model validation in the preceding sections, the experimental data were frequently identified with and analyzed in terms of volume reduction factor at saturation, which is essentially the cumulative feed volume fed to the pot in multiples of pot volume, until the solution just becomes fully saturated. However, the VRF model was developed specifically for the 80% saturated solutions, since the target endpoint for the actual evaporator operation would be more like 80% saturation rather than 100% saturation so that any potential for forming solids during storage and/or transfer would be precluded.

Despite its usefulness in actual plant operation, the VRF model could not be validated in this work, since it is not possible to determine the 80% saturation point experimentally. Instead, the most that can be done to validate the VRF model is to make qualitative assessments based on the fact that measured VRFs at 100% saturation should be higher than those predicted at 80% saturation. It is the question of how much higher that cannot be addressed in this work.

Both measured and predicted VRFs that were presented in the previous section are compared in Table 2-19. As expected, the predicted VRFs at 80% saturation for the AN-102, AN-103, and AN-107 samples are lower than the measured data for the respective samples at 100% saturation. However, the absolute difference ranging from 0 to 11% between the predicted and measured VRFs for the AN-102 sample appears to be too small. For the remaining AW-101 and AZ-102 samples, the model is shown to greatly over predict the measured VRFs. Based on these conflicting results, it is therefore recommended that the VRF model in its current form not be used to predict the evaporator endpoint of 80% saturation to support plant operation.

Table 2-19. Comparison of Volume Reduction Factors

	Predicted VRFs	Measured VRFs		Predicted - Measured
Sample	@ 80% Saturation	@ Pre-Precipitation	@ Post-Precipitation	% Measured VRFs
AN-102	39	40	44	-11 to 0
AN-103	39	56	64	-30 to -39
AN-107	73	86	94	-15 to -22
AW-101	20	14	16	25 to 43
AZ-102	54	40	50	8 to 35

This page intentionally left blank.

3.0 FUTURE WORK

Comparison of the predicted bulk solubility values and the experimental data suggests that the negative bias of the model is on the order of 10%. Since the calculations were 4 to 21% low, a 10% shift in the bias would place all of the model predictions within ±10% of the experimental data, thus satisfying the task acceptance criterion. As discussed in Section 2.3.4, this negative bias of the solubility model is thought to be partly due to the questionable prediction by the 6-component nitric acid database used in this work on the partitioning of total acid between dissociated and undissociated acids. Consequently, additional database and modeling work is recommended to identify and correct the source of this apparent bias in the solubility model.

This page intentionally left blank.

4.0 REFERENCES

Choi, A. S., and Barnes, C. D., 2001a, "Task Technical and Quality Assurance Plan for Cesium and Technetium Eluate Physical Property Modeling," **WSCR-TR-2001-00408, Rev. 0**, Westinghouse Savannah River Co., Aiken, SC.

Choi, A. S., 2001b, "Software Quality Assurance Plan for Hanford RPP-WTP Evaporator Modeling," **WSRC-RP-2001-00337, Rev. 0**, Westinghouse Savannah River Co., Aiken, SC.

Choi, A. S., 2001c, "Estimation of Physical Properties of AN-107 Cesium and Technetium Eluate Blend," **WSCR-TR-2000-00527**, Westinghouse Savannah River Co., Aiken, SC.

Choi, A. S., Edwards, T. B., and Pierce, R. A., 2003, "Physical Property Models of Concentrated Cesium Eluate Solutions," **WSCR-TR-2002-00424, Rev. 0**, Westinghouse Savannah River Co., Aiken, SC.

ESP Software, http://www.olisystems.com/, OLI Systems, Inc., Morris Plains, NJ (2002).

Hassan, N. M., and McCabe, D. J., 1997, "Hanford Envelope B Tank Waste Ion Exchange Column Study (U)," **SRTC-BNFL-019, Rev. 0**, Westinghouse Savannah River Co., Aiken, SC.

Hassan, N. M., Adu-Wusu, K., and Nash, C. A., 2003, "Multiple Ion Exchange Column Runs for Cesium and Technetium Removal from AW-101 Waste Sample (U)," **WSRC-TR-2003-00098,** Westinghouse Savannah River Co., Aiken, SC.

Kurath, D. E., Blanchard, D. L., and Bontha, J. R., 2000, "Small Column Ion Exchange Testing of Superlig 644 for Removal of 137Cs from Hanford Tank Waste Envelope A (Tank 241-AW-101)," **BNFL-RPT-014, Rev. 0**, Pacific Northwest National Laboratory, Richland, WA.

Longwell, R. L., 2001, "Eluate Physical Properties and Evaporation Test Specification," **24590-WTP-TSP-RT-01-008, Rev. 0**, Washington Group International, Richland, WA.

Olson, J. W., 2001, "System Description for Cesium Removal Using Ion Exchange – System CXP," **24590-PTF-3YD-CXP-00001**, **Rev. A**, Bechtel National, Inc., Richland, WA.

Perry's Chemical Engineering Handbook, 6th Ed., R. H. Perry and D. Green, Eds., McGraw-Hill, New York (1984) p. 3-252.

Pierce, R. A., 2002, "Cesium Eluate Evaporation Solubility and Physical Property Behavior," **WSRC-TR-2002-00411, Rev. 0**, Westinghouse Savannah River Co., Aiken, SC.

Pierce, R. A., 2003, "Cesium Eluate Semi-Batch Evaporation Performance," **WSRC-TR-2003-00135, Rev. 0**, Westinghouse Savannah River Co., Aiken, SC.

Woodworth, M., 2002, "System Description for Cesium Nitric Acid Recovery Process – System CNP," **24590-PTF-3YD-CNP-00001**, **Rev. B**, Bechtel National, Inc., Richland, WA.

This page intentionally left blank.

APPENDIX A. SAMPLE CALCULATIONS

Prediction of the Physical Properties of Radioactive AW-101 Cesium Eluate

The scaled weight fractions of the six major cations, not including the other minor species, are given in Table 2-11. This composition was entered into Equation 2-1 along with *Temp* = 20 ^{o}C for each physical property estimation as follows:

Volume Reduction Factor at 20 ^{o}C:

$$\begin{aligned} VRF &= (139.01782)(0.05) + (48.97029)(0.001) + (27.90272)(0.032) \\ &= + (63.09169)(0.129) + (54.90814)(0.136) - (11.80459)(0.652) \\ &\quad + \begin{bmatrix} (-3.30647)(0.05) + (-1.07174)(0.001) + (0.58164)(0.032) \\ + (7.73972)(0.129) + (-0.48689)(0.136) + (0.52935)(0.652) \end{bmatrix}(20) \\ &= 38 \end{aligned}$$

Density at 100% saturation and 20 ^{o}C:

$$\begin{aligned} \rho_{20\,C}^{sat} &= (1.48886)(0.05) + (1.47408)(0.001) + (1.50460)(0.032) \\ &= + (1.31406)(0.129) + (1.42237)(0.136) + (1.25453)(0.652) \\ &\quad + \begin{bmatrix} (-0.00619)(0.05) + (-0.00111)(0.001) + (0.00147)(0.032) \\ + (0.00142)(0.129) + (0.00209)(0.136) + (0.00240)(0.652) \end{bmatrix}(20) \\ &= 1.3403 \ \ g/ml \end{aligned}$$

Bulk Solubility at 20 °C:

$$\begin{aligned} S_{20\,C} &= (0.73699)(0.05) + (0.74161)(0.001) + (0.69789)(0.032) \\ &= +(0.51292)(0.129) + (0.77862)(0.136) + (0.42178)(0.652) \\ &\quad + \begin{bmatrix} (-0.01693)(0.05) + (-0.00097)(0.001) + (0.00599)(0.032) \\ +(0.00356)(0.129) + (0.00590)(0.136) + (0.00559)(0.652) \end{bmatrix}(20) \\ &= 0.5920 \ \ g\,TS/ml \end{aligned}$$

Viscosity at 100% Saturation at 20 °C:

$$\begin{aligned} \mu_{20\,C} &= (12.72718)(0.05) + (4.95164)(0.001) + (3.95236)(0.032) \\ &= +(2.14149)(0.129) + (2.5131)(0.136) + (1.38919)(0.652) \\ &\quad + \begin{bmatrix} (-0.07447)(0.05) + (-0.09208)(0.001) + (-0.02821)(0.032) \\ +(-0.00294)(0.129) + (0.00172)(0.136) + (0.00758)(0.652) \end{bmatrix}(20) \\ &= 2.2931 \ \ cP \end{aligned}$$

Heat Capacity at 100% Saturation at 20 °C:

$$\begin{aligned} Cp_{20\,C} &= (-0.03378)(0.05) + (0.38964)(0.001) + (0.49192)(0.032) \\ &= +(0.84166)(0.129) + (0.4644)(0.136) + (0.83926)(0.652) \\ &\quad + \begin{bmatrix} (0.00287)(0.05) + (0.00499)(0.001) + (0.00185)(0.032) \\ +(-0.0059)(0.129) + (0.00039)(0.136) + (-0.00426)(0.652) \end{bmatrix}(20) \\ &= 2.2931 \ \ cP \end{aligned}$$